

## IMAGING PROPERTIES OF AN HYPERTELESCOPE

Patru, F.<sup>1</sup>, Mourard, D.<sup>1</sup> and Lardière, O.<sup>2</sup>

**Résumé.** In the future, optical stellar interferometers are going to provide true images, by increasing the number of telescopes and by cophasing the beams. Then it is time to study the future large array using the hypertelescope mode for direct imaging applications. Numerical simulations have been performed to study the direct imaging properties. It is shown that the choice of the geometry of the array is a trade-off between the resolution, the dynamic, the field of view and the astrophysical objectives. A regular and unredundant pattern of the input pupil optimizes the dynamic, the contrast and the accuracy of the densified image, but decreases the useful field of view. A spotted star, with a low contrast, requires dynamic, whereas a large field is suitable for the multiple stars.

### 1 Introduction

Future large interferometers require a large number of telescopes and an active cophasing system, to provide images with sufficient sensitivity. If both conditions are achieved, snapshot imaging can be produced with the hypertelescope mode. With a large number of beams, a multi-axial assembly seems to be the best solution, compared to the pairwise combiner currently used for optical aperture synthesis. If the entrance pupil is highly diluted, the hypertelescope mode (Labeyrie 1996) improves the Fizeau mode (Fizeau 1868), with a high sensitivity gain without loss of field of view (Lardière 2007).

This paper summarizes the numerical simulations developed for that purpose Patru 2007, Patru 2008, the question being how to optimize the imaging capabilities of an hypertelescope. For that, we have developed an IDL program, called HYPERTEL, which simulates and analyzes direct images.

### 2 Description of the PSF

The densification increases the relative size of the beams by preserving the relative positions of the sub-pupil centers. This pseudo-homothetic transformation does not affect the interference function to reconstitute high resolution information, whereas the diffraction envelope is reduced, so as to focus all the flux in the useful field and to intensify the signal by a factor  $\gamma^2$  (Fig. 1).

The PSF intensity distribution of an hypertelescope can be generally written as (Lardière 2007)

$$PSF(x, y) = A(x, y) \cdot I_0(x, y) \quad (2.1)$$

The PSF is the product of the interference function of the array  $I_0(x, y)$  by a diffraction envelope  $A(x, y)$  function of the beam combiner (Fig. 1). The envelope width decreases as the densification factor increases. The interference function is formed by 2 parts : a central peak with a halo of side-lobes due to the holes in the entrance pupil, and a diffused halo of speckles due to the space aliasing effect corresponding to the lower spatial frequency  $\lambda/s$  sampled by the array. The field beyond  $\lambda/s$  is aliased in the interference function (Aime 2006).

The Clean Field of view (CLF), or useful field, is the central part of the PSF where the halo contribution is negligible, i.e. where the halo is due to the side-lobes and is not affected by the space aliasing effect. The angular radius of the clean field equals to  $CLF = \lambda/s$  (Lardière 2007).

---

<sup>1</sup> Observatoire de la Côte d'Azur, Dpt. Gemini, UMR 6203, F-06130 Grasse, France

<sup>2</sup> Adaptive Optics Lab, Engineering Lab Wing B133, University of Victoria, PO Box 3055 STN CSC, Victoria, BC, Canada V8W 3P6

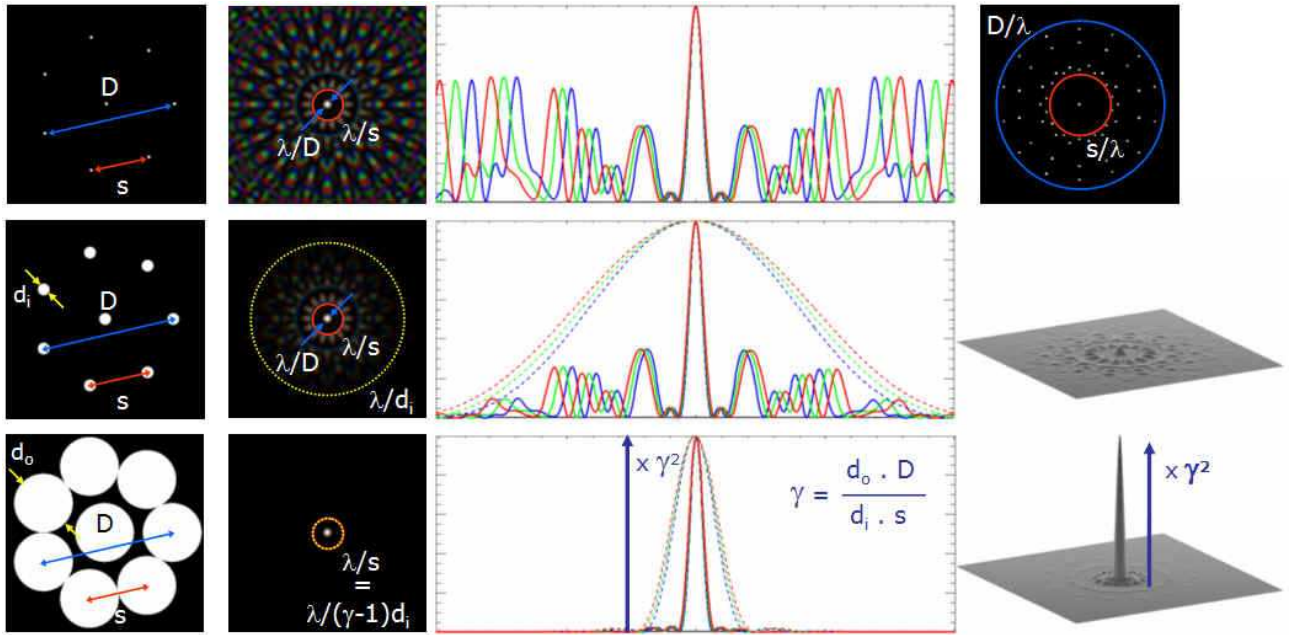


**Fig. 1.** Field of view definition in direct imaging. Interference function without diffraction envelope (up), Fizeau PSF (middle) and densified PSF (down) obtained with an array of 8 telescopes. In each case, the corresponding pupils are shown on the left side. At the top right corner the  $(u,v)$  plan coverage is given ; the spatial frequencies in the hypertelescope mode are distributed on the interval  $[s/\lambda, D/\lambda]$ , with  $s$  the smallest baseline and  $D$  the largest baseline of the array. The interference function corresponds to the image obtained with unresolved aperture. The intensity distribution is intrinsic to the array, and its extension is infinite by definition. We observe a central peak inside a clean zone, called the Clean Field (*CLF*), where the contribution of the halo of side-lobes is minor. The central peak width equals to a fraction of one resel  $\lambda/D$ . It is surrounded by a non-negligible halo of speckles outside the *CLF* diameter  $\lambda/s$ . In practice, the interference function is multiplied by an envelope function (dotted lines). The Fizeau PSF is limited by the Airy envelope of an input sub-aperture, which corresponds to the coupled field ( $CF = \lambda/d_i$ ). The pupil densification reduces the envelope width so as to equalize the Direct Imaging Field ( $DIF = \lambda/((\gamma - 1) d_i)$ ) with the *CLF*, and so as to gain in sensitivity by a factor  $\gamma^2$  and without a loss of useful field of view.

To characterize the PSF quality, we consider here the encircled energy  $E_0/E_{tot}$  as the ratio of the fraction of energy contained in the central peak on the total energy in the image. The encircled energy is an estimator of the spread light effect in the side-lobes.

### 3 Influence of the geometry of the array

We consider 4 types of configurations of large arrays, defined by (Lardière 2007) : ELSA (Quirrenbach 2004), OVLA (Labeyrie 1986), KEOPS (Vakili 2004) and CARLINA (Le Coroller 2004). The figure 2 gives the characteristics of the densified PSF of arrays of 40 telescopes.

For a given resolution (same maximal baseline), there is a trade-off between dynamic and field. OVLA is suitable to image large and low contrasted field, by using relatively short baselines. KEOPS is optimized for high contrast imaging, thanks to a regular and non redundant layout of the telescopes of the array. The KEOPS configuration is well adapted for imaging, because the pupil is uniform (the interference function is similar to an Airy function) and non redundant (the halo is uniform). The entrance pupil must be optimized with a uniform coverage where the telescopes are regularly spaced. If the densified pupil is practically filled, the central part of the interference function is very similar to the diffraction function of an equivalent giant telescope which covers the output sub-pupils.

For a given configuration, there is a trade-off between resolution and field. The resolution is improved by increasing the global size of the input pupil ( $D$ ). As the pupil is more diluted, the clean field is decreased. A

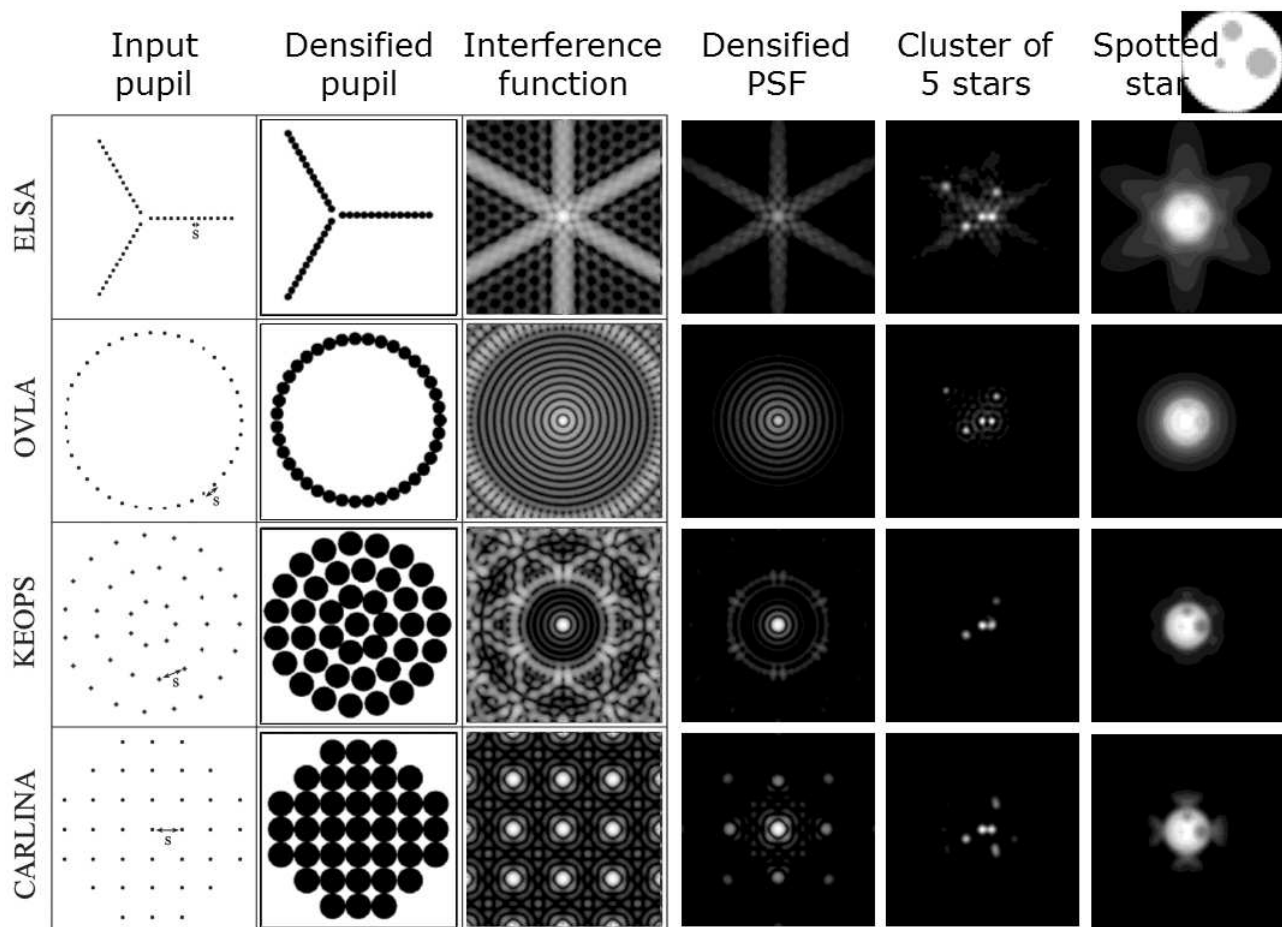


**Fig. 2.** Imaging properties of 4 array configurations. From left to right : entrance pupil of the array, densified output pupil, interference function of the array, densified PSF, application to a cluster of 5 iso-photometric stars, application to a resolved star with 3 spots. ELSA and OVLA provide a large Clean Field weakly contrasted, whereas KEOPS and CARLINA provide a higher dynamic in a lower field. OVLA is suitable for a cluster of unresolved stars, whereas KEOPS is required for stellar surface imaging.

compact array provides a large image with low resolution and a diluted array provides a narrow image with high resolution. The only variable parameter is the angular scale on the sky (size of the resel and size of the clean field), whereas the number of resels remains the same ( $N_{resels} = D/s$ ). It is interesting to benefit from a movable array with a fixed geometry like KEOPS and with a sufficient number of telescopes. The telescopes are moved so as to keep the same geometry and to equalize the clean field with the object.

As a general rule, the choice of the geometry of an array is a trade-off between resolution, field and dynamic.

#### 4 Application to astrophysical objectives

Firstly, we consider the snapshots of 5 stars with the same photometry (Fig. 2). KEOPS provides the best restitution of the stellar parameters : photometries ( $< 1\%$ ) and diameters ( $< 1\%$ ) of the stars, separations ( $< 3\%$ ) between them. But the narrow field limits this configuration to the study of compact systems as a closed binary. OVLA is interesting with a large clean field which is suitable for large stellar clusters. In return, a degradation is observed on the intensity ( $< 25\%$ ) and on the diameter ( $< 15\%$ ), while the relative positions of the stars are well-preserved ( $< 3\%$ ).

Secondly, we consider the snapshots of a star with 3 spots on its surface (Fig. 2). It is clear that the restitution of the spots is better with KEOPS or CARLINA than with OVLA or ELSA. The contrast is important for

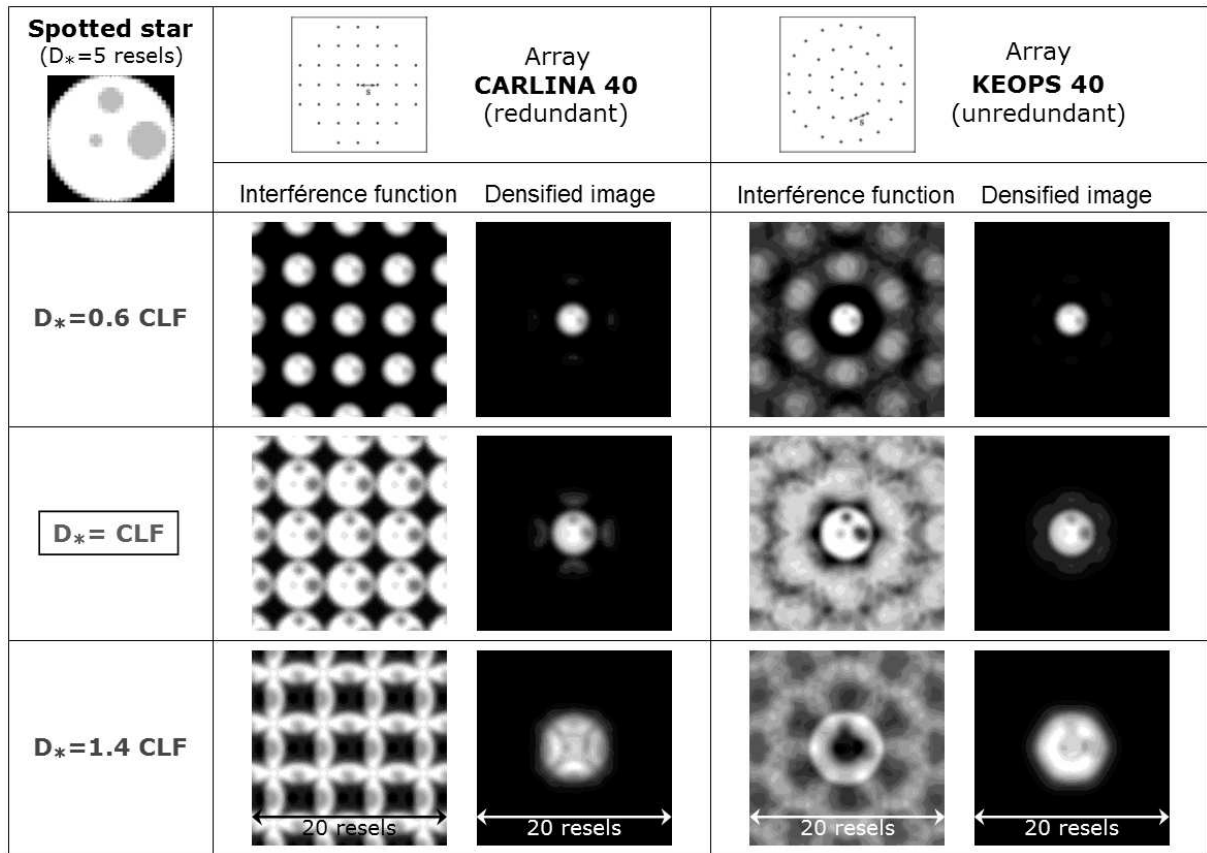


**Fig. 3.** Influence of the diameter of the object as a function of the size of the clean field. The spotted star has a diameter equal to 0.6 time (up), 1 time (middle) and 1.4 time (down) the diameter of the clean field, in the case of the configurations CARLINA40 (redundant case) and KEOPS40 (unredundant case). The star smaller than the clean field is weakly resolved, so that the smallest spot is unresolved. The star higher than the clean field is saturated, because of the space aliasing effect of the interference function. The problem persists whatever the densification level. The required condition is to adapt the size of the clean field to the size of the object.

imaging extended objects for two reasons. The first one is that the spots contrast on a giant star is very low ( $\approx 10^2$ ), although less critical in the visible. The second one is that the image is smoothed by the diffraction effects. Each point of the stellar surface is convolved by the PSF, which implies a contribution of the halo. This halo will be reimaged around each point of the image. The superposition of all these halos involves a global contrast drop in the image. KEOPS provides the best dynamic and thus restores the highest contrast.

The sine qua non condition to image properly a star is that the star diameter remains lower than the clean field diameter  $\lambda/2s$ . In the same way, the image of a stellar surface is optimal if the star diameter equals to the size of the clean field :  $D_{obj} \approx \lambda/s$  (Fig. 3). A lower star is under-sampled, whereas a higher star is saturated due to the space aliasing effect. It shows that the real imaging field is a function of the array, and no of the recombination mode.

To clarify, remember that the PSF is the interference function multiplied by the envelope. The densification process never affects the interference function. If the clean field is already polluted by coupled objects (outside the clean field and inside the coupled field), the interference function is biased, whatever the densification level, i.e. whatever the width of the diffraction envelope.

## 5 Restoration of the astrophysical parameters

Regarding the snapshot imaging (without any post-treatment), the photometric parameters (amplitude) are more difficult to restore than the astrometric parameters. Four main effects are distinguished :

- the bias of the interference function,
- the bias of the diffraction envelope,
- the bias of space aliasing,
- the bias of crowding.

The bias of the interference function, the bias of space aliasing and the bias of crowding depend on the array configuration. The bias of the diffraction envelope is only linked to the recombination mode.

### 5.1 Bias of the interference function

The quality of the interference function of the array determines the residual halo level. If the input sub-pupils are distributed homogeneously, the halo inside the clean field reproduces the interference function of a large array covering all the sub-pupils. If the entrance pupil shows gaps, additional diffraction figures are added to first one. The astrometric parameters are weakly disturbed, contrary to the photometric parameters which are biased by the halo.

In the case of two narrow unresolved sources, the energy of the side-lobes are added to the energy of the main peaks. A photometry of the star is not the same if it is closed to or far away another one. In the case of an extended source like a stellar surface, each point of the object gives locally a diffraction peak with surrounding a halo. The overlap of all these peaks smooths the image, which induce a contrast loss.

The halo is minimized by maximizing the densified pupil filling rate, defined as the ratio of the total surface of the densified sub-pupils by the surface of the giant telescope inscribed around the sub-pupils (Patru 2008). An optimized array should provide a regular pattern of the sub-apertures in the entrance pupil. Note that the apodization techniques should remove the halo (Aime 2003a).

### 5.2 Bias of the diffraction envelope

Due to the diffraction envelope contribution, which is a Bessel function in DP mode, the photometry decreases from the axis to the edge of the clean field. This effect is critical with a maximal densification. A partial densification restitutes a more homogeneous photometry on the clean field. This bias does not exist in IRAN mode, where the envelope is flat, which should simplifies the deconvolution work.

The influence of the recombination mode and the level of densification is discussed by Patru 2008.

### 5.3 Space aliasing effect

The space aliasing effect (Aime 2006), or coupling effect, occurs when the science object is surrounded by other stars inside the coupled field and outside the clean field, or when the science object diameter goes over the clean field. This effect remains the same whatever  $\gamma$ . Indeed, the quality of the clean field is polluted by other stars in the coupled field, in Fizeau mode, as in DP mode, as in IRAN mode. The densification intensifies the central peak and the lobes by the same factor.

In other words, the direct imaging is well adapted for compact and isolated objects, whatever  $\gamma$ . The science object do not have to exceed the clean field diameter, and the coupled field do not have to be filled by many surrounding stars. The coupled field is problematic for low bright stars. The risk to find other low magnitude stars inside the coupled field becomes rapidly drastic.

### 5.4 Crowding effect

The crowding limit says that a non redundant array of  $N_T$  telescopes provides approximatively an image of  $N_T \times N_T$  resels. The crowding effect is critical when the information field is poor and when the object is complex. On the whole, the crowding effects induces a contrast loss. If the crowding limit is reached, the clean field becomes photometrically uniform, so that the high resolution information is lost.

The crowding limit depends not only on the number of telescopes, but also on the size of the coupled field. When the coupled field increases, the risk to couple objects in the clean field increases also, and the image will be more saturated up to the crowding limit.

The influence of the number of telescopes is discussed by Patru 2008.

### 5.5 Methods of post-treatment

All these biases can be corrected in principle by the techniques of post-treatment. A first idea is that the diffraction envelope in DP mode is well known and can be compensated by soft. The diffraction envelope is extracted as a flat-field, but the edge of the image is degraded compared to the center part, depending on the signal to noise ratio.

The CLEAN method (Högbom 1974) is well suited to analyze a multiple stellar system. The shape of the central peak and the side-lobes are taken into account by a convolution of each peak by the PSF. Then, the peak is extracted from the "dark map" at same time as the surrounding halo.

The deconvolution technics is required for more complex objects. In the case of a densified image, the problem is that the convolution relationship in Fizeau is lost. The image is partially truncated, which means that it is reduced to a finite support, the direct imaging field. When  $\gamma$  increases, this support becomes narrower. This partial lack of data are lost after convolution of the object by the PSF. The PSF is also truncated, which is a problem for the classical methods of deconvolution. To overcome this problem, it exists an hybrid method, based on likelihood maximization, which reconstructs simultaneously the object and the PSF (Aristidi 2005).

It is a priori more difficult to deconvolve a densified image compared to a Fizeau image, supposing a low signal to noise ratio. A variable densification can facilitate the efficiency of the deconvolution. There is a trade-off between increasing  $\gamma$  to improve the signal to noise ratio, and decreasing  $\gamma$  to limit the reduction of the support of information.

## 6 Conclusion

These studies are placed in the long term prospecting for future large interferometers. Simulations have shown that the choice of the array configuration is a trade-off between the resolution, the dynamic, the useful field and the astrophysical goals. The best adapted configuration should have a regular and non redundant layout of the telescopes to maximize the densified output pupil filling rate. The densified pupil is uniform (central peak similar to the Airy function) and non redundant (uniform halo).

The direct imaging technique has already an interest for current interferometers, by using an efficient cophasing system and a specific deconvolution algorithm. The densification provides an ultimate sensitivity, which is required to observe weak objects so as to enlarge the sky coverage in stellar interferometry, and to open new astrophysical highlights, as the stellar surface structures. Next studies will compare the imaging performances and applications between direct imaging and aperture synthesis imaging.

## Références

- Aime C., Soummer R. 2003, *Astronomy with High Contrast Imaging*, EAS Publications Series, 8, 79  
 Aime C. 2003, *Astronomy with High Contrast Imaging*, EAS Publ. Ser., 22, 351  
 Aristidi E. et al. 2005, *EAS Publications Series*, 12, 103  
 Fizeau A.H. 1868, *C.R. Acad. Sci. Paris*, 66, 932  
 Högbom J.A. 1974, *A&As*, 15, 417  
 Labeyrie A. et al. 1986, *Proc. SPIE*, 628, 323  
 Labeyrie A. 1996, *A&A Suppl. Ser.*, 118, 517  
 Lardièrre O. et al. 2007, *Mon. Not. R. Astron. Soc.* 375, 977  
 Le Coroller H. et al. 2004, *A&A*, 426, 721  
 Patru F. 2007, Ph.D. Dissertation, Université de Nice Sophia-Antipolis  
 Patru F. et al. 2008, in preparation  
 Quirrenbach A. 2004, *Proc. of the 37th Liege International Astrophys. Coll.*, 43  
 Vakili F. et al. 2004, *Proc. SPIE*, 5491, 1580